

1 **Adsorption of clofibric acid on the activated carbon prepared**
2 **from polyester cloth waste: Study of the operational parameters,**
3 **kinetics and adsorptive equilibrium using the non-linear method**

4 NASSIMA BOUDRAHEM-BOUALIT^{1-3*}, NABIL MAMERI³ and MOUNA CHALA¹

5 ¹Laboratoire des Sciences et Techniques de l'Environnement, Ecole Nationale Polytechniques
6 Alger, Avenue Pasteur El Harrach, 16110 Alger, Algeria, ²Faculté de Technologie, Université
7 de Bejaia, Bejaia 06000, Algeria and ³Laboratoire de biotechnologie, Ecole Nationale
8 Polytechniques Alger, Avenue Pasteur El Harrach, 16110 Alger, Algeria

9 (Received 15 May, revised 25 June, accepted 6 August 2025)

10 *Abstract:* The objective of this research work was to examine the feasibility of
11 preparing adsorbent materials from textile waste (polyester) for the elimination
12 of pharmaceutical products such as clofibric acid (CA). The results showed that
13 the adsorbents prepared by chemical activation in the presence of phosphoric
14 acid followed by pyrolysis at 600 °C led to microporous materials with large
15 specific surfaces. Batch experiments were conducted to study the effect of con-
16 tact time, initial CA concentration, solution pH and temperature. Elimination
17 yields by adsorption of CA in aqueous solution greater than 95 % were obtained
18 with dilute solutions (10 mg L⁻¹) at room temperature and at pH 3. The ads-
19 orption kinetics is perfectly described by the pseudo-second-order model and the
20 isotherms are of the Freundlich types. The results indicate that this process is
21 spontaneous, efficient and potentially applicable in the removal of CA from water.

22 *Keywords:* activated carbon cloth; pharmaceutical active compounds; waste
23 water; H₃PO₄.

24 INTRODUCTION

25 Pharmaceutical active compounds (PhACs) are a class of emergent pollutants
26 that are being continuously introduced into the environment mainly due to im-
27 proper disposal of unused or expired drugs and through excretion and inefficient
28 removal in sewage treatment plants (STPs).¹ Even though the amounts found in
29 the environment are usually low (they are often detected in trace concentrations
30 (ng L⁻¹), long-term exposure of aquatic and terrestrial organisms may provoke
31 adverse effects on respective ecosystems.² Some of these compounds such as
32 carbamazepine, clofibric acid, diclofenac, tetracycline, paracetamol and caffeine

* Corresponding author. E-mail: nassima.boudrahem@g.enp.edu.dz
<https://doi.org/10.2298/JSC250515063B>

33 have shown persistent behavior, which may lead to their bioaccumulation when
34 present in the environment. Moreover, the degradation of some drugs can produce
35 highly toxic and carcinogenic compounds.

36 It is thus important to remove all these pharmaceutical products from waste-
37 water and this can be done using electrochemical methods, membrane filtration,
38 adsorption, biodegradation and advanced oxidation processes (AOPs). Compared
39 with the above methods, adsorption is considered as a promising method for rem-
40 oving various pollutants from wastewater due to its economical, renewable, and
41 flexible operation.³

42 Activated carbon cloths (ACCs) present technological advantages over more
43 traditional powder or granular forms of activated carbons, including high adsorp-
44 tion capacity, uniform porosity and high rates of adsorption/desorption from the
45 gas or liquid phase, as well as new applications such as molecular sieves, catalysts
46 and electrodes.^{3,4} The textural and chemical characteristics of activated carbon
47 depend on the nature of the precursor used as well as the methods and conditions
48 of production.⁵ Currently, the major precursors for producing ACC include syn-
49 thetic materials such as acrylic, nylon and polyester fibres and natural materials
50 such as wool, flax, viscose and cotton.³ The preparation of activated carbon from
51 polyester woven waste, similar to that of conventional activated carbon, involves
52 its treatment by physical or chemical activation processes.⁶

53 Some researchers have shown ACCs' efficiency in aqueous media for the rem-
54 oval of organic and inorganic compounds for example Brasquet *et al.*⁷ examined
55 the quantitative structure–property relationship for the adsorption of 55 organic
56 compounds onto activated carbon cloth. Brasquet and Cloirec⁸ studied the effects
57 of activated carbon cloth surface properties on organic adsorption in aqueous sol-
58 utions. Ayranci and Dumain⁹ evaluated the adsorption capacity of ACCs vis-a-vis
59 of phenolic compounds (phenol, hydroquinone, *m*-cresol, *p*-cresol and *p*-nitro-
60 phenol). Adsorption of cadmium by activated carbon cloth based on polyacrylo-
61 nitrile fibre as a precursor was oxidised using nitric acid, ozone and electrochem-
62 ical oxidation has been reported by Rangel-Mendez and Streat.¹⁰ Álvarez-Merino
63 *et al.*¹¹ investigated the adsorption of Zn(II) ions from aqueous solution under
64 static conditions using commercial activated carbons in the form of grains and
65 cloth. Akkouche *et al.*¹² studied the adsorption of tetracycline and paracetamol
66 from aqueous solutions using activated carbon derived from cotton textile waste
67 modified with H₃PO₄. Boudrahem *et al.*³ studied the adsorption of clofibric acid
68 from aqueous solutions using activated carbon derived from cotton textile waste
69 activated with H₃PO₄.

70 In this work we investigated the feasibility of using polyester cloth waste as
71 precursor for the production of activated carbons with activation by H₃PO₄. The
72 physicochemical properties of ACs, such as BET surface area, morphology and
73 surface functional groups, were analyzed to better understand the mechanism of

74 adsorption of clofibric acid (2-(*p*-chlorophenoxy)-2-methylpropionic acid, CA).
75 The effects of initial concentration of the adsorbate, pH of the solutions, contact
76 time and temperature were evaluated. Moreover, different adsorption isotherm
77 models, including Langmuir and Freundlich were used to analyze the adsorption
78 equilibrium data. Pseudo-first and pseudo-second order models were used to study
79 the kinetic process.

80 The choice of textile waste in this study is linked to its great availability, its
81 low cost and the need to preserve natural resources for future generations. For
82 example, it is estimated that the production of textile waste in Algeria in the year
83 2014 was 1,430,000 t. As for the choice of the target molecule (clofibric acid), this
84 is due to its belonging to a class of consumer products, to its presence in the env-
85 ironment and its specific action on microorganisms.

86 EXPERIMENTAL

87 *Materials*

88 Polyester cloth waste used in this study was obtained from a clothing production factory
89 (ALCOST-Bejaia-Algeria). Nitrogen gas was industrial grade of 99 % purity. The reagent grade
90 chemicals used in the study (H_3PO_4 , H_2SO_4 , HCl, NaOH) and clofibric acid (CA), were
91 purchased from Aldrich and Junsei chemical companies.

92 *Preparation of the activated carbon (AC)*

93 Polyester cloths residues were used as a precursor for the preparation of AC. The cloths,
94 previously weighed, were immersed in the H_3PO_4 solution for 7 h at 85 °C to ensure the access
95 of the activating agent to the interior of the precursor, and then the temperature of the mixture
96 was increased and maintained at 100 °C until it was completely dry. Three activation ratios, 25,
97 50 and 75 wt. % (wt = mass of H_3PO_4 /mass of precursor) were tested. The dried samples were
98 pyrolyzed at 600 °C for 1h under an inert gas stream (N_2 flow). The heating rate was 10 °C min^{-1} .
99 The AC samples were cooled down to room temperature while still under N_2 flow. Afterwards,
100 the resulting activated carbons were rinsed thoroughly with distilled hot water until a neutral
101 pH was obtained in order to remove all acid, then dried and kept in a desiccator before use.

102 *Characterization of the AC prepared*

103 The surface area, micropore volume and pore size distribution were determined using the
104 nitrogen adsorption isotherm technique measurements at the liquid nitrogen temperature of 77
105 K (Micromeritics Instrument Corporation MicroActive Tristar II 3020).

106 The surface morphology of ACs was examined by scanning electron microscopy
107 (SEMJSM820, Jeol Ltd., Japan).

108 The surface chemical properties of the samples were characterized by the Fourier-trans-
109 form infrared spectroscopy (Shimadzu FTIR-8300, Japan) at room temperature. The spectra
110 were recorded in the 4000–400 cm^{-1} wavenumber range.

111 The carbon surface charge is mainly determined by the pH of the adsorbate solution. The
112 pH at the point of zero charge (pH_{PZC}) of the carbon was determined using the method reported
113 by Khenniche and Aissani.¹³

114 *Batch adsorption procedure*

115 Adsorption experiments were carried out by mixing 0.25 g of ACs with 250 mL of each
116 clofibric acid solution (10 to 100) $mg L^{-1}$ in a batch reactor (500 mL) under the following

117 conditions: 360 rpm stirring speed, 3 h contact time, temperature, 20, 30, 40 and 50 °C, and
 118 desired initial pH value of the solution. The concentration of the clofibrac acid was measured
 119 using a UV–Vis spectrophotometer at a wavelength of 227 nm. The CA adsorption capacity at
 120 time t , q_t , was evaluated using as:

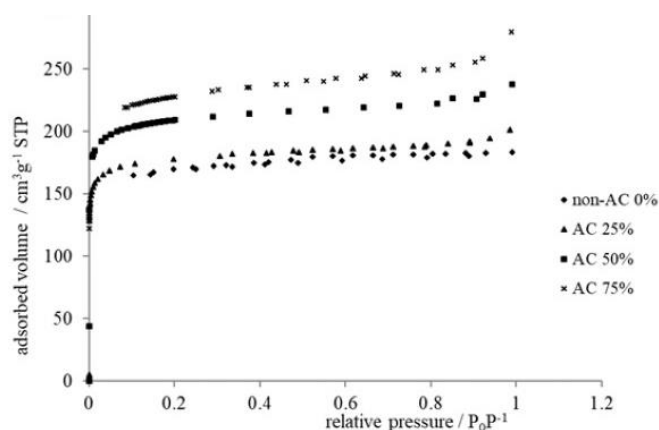
$$121 \quad q_t = \frac{(C_0 - C_t)V}{m} \quad (1)$$

122 in which q_t is the adsorption capacity at time t (mg g^{-1}), C_0 (mg L^{-1}) is the initial concentration
 123 of CA, C_t (mg L^{-1}) is the concentration of CA at time t , V (L) is the volume of the CA solution
 124 and m (g) is the mass of the ACs. At the equilibrium: $q_t = q_e$ and $C_t = C_e$.

125 RESULTS AND DISCUSSION

126 *Optimization of adsorbent characteristics*

127 *Nitrogen adsorption – textural characteristics.* Before attempting to obtain
 128 quantitative information, a study of the form and textural characteristics was imp-
 129 posed. Nitrogen adsorption–desorption isotherms were plotted for the various ads-
 130 orbents prepared by plotting the amount of nitrogen adsorbed or desorbed per g of
 131 adsorbent as a function of relative pressure. The results presented in Fig. 1 show
 132 that all nitrogen adsorption isotherms are type I (Langmuir isotherm) according to
 133 the IUPAC classification.¹⁴ This type of isotherm suggests that the adsorbents are
 134 of the microporous type. This result was confirmed by the desorption isotherm.
 135 The speed of reaching the plateau is an indication of the pore size distribution and
 136 the presence of the horizontal plateau suggests a very low external surface area.



137
 138 Fig. 1. Adsorption–desorption isotherms of nitrogen at 77 K of ACs with different H_3PO_4
 139 impregnation ratios.

140 The physical properties results obtained from the N_2 adsorption–desorption
 141 isotherms of all ACs were determined and reported in Table I.

142 Analysis of the Table I data reveals that activated carbons prepared from poly-
 143 ester are characterized by large specific surface areas. The activation increases the

144 S_{BET} , V_t , V_{mic} and V_{mes} . The microporosity ratio (V_{mic}/V_t), %, of the adsorbents
 145 prepared decreases with the impregnation ratio, decreasing from 99.74 % for non-
 146 -activated carbon 0 % H_3PO_4 to 98.6 % for an activation rate of 75 % H_3PO_4 . We
 147 have noticed in this case the development of mesoporosity. This effect may be due
 148 to the hydrolysis of the polyester during the impregnation with the acid, which
 149 means an important release of volatile compounds during the heat treatment.¹⁵
 150 These results are confirmed by Ramos *et al.*,¹⁵ showing that the use of phosphoric
 151 acid as an activating agent not only contributes to the creation of new micropores
 152 but also to the enlargement of the pores already existing in the precursor.

153 TABLE I. Physicochemical properties of activated carbons

Parameter	Impregnation ratio with H_3PO_4			
	AC 0 %	AC 25 %	AC 50 %	AC 75 %
$V_{\text{tot}} / \text{cm}^3 \text{g}^{-1}$	0.271	0.335	0.285	0.369
$V_{\text{mic}} / \text{cm}^3 \text{g}^{-1}$	0.271	0.326	0.274	0.363
Microporosity, $V_{\text{mic}}/V_{\text{tot}}$ in %	99.74	97.41	96.18	98.6
$V_{\text{mes}} / \text{cm}^3 \text{g}^{-1}$	0.00072	0.0087	0.011	0.0052
Mesoporosity, $V_{\text{mes}}/V_{\text{tot}}$ in %	0.264	2.591	3.819	1.4
$S_{\text{BET}} / \text{m}^2 \text{g}^{-1}$	415.45	776.23	534.08	826.2
$S_{\text{ext}} / \text{m}^2 \text{g}^{-1}$	89,17	101.21	75.92	152.2
$S_{\text{mic}} / \text{m}^2 \text{g}^{-1}$	326.28	675.02	458.16	674
$d_p = 4V_{\text{tot}}/S$ in Å	26.13	17.25	21.32	17.85
pH_{PZC}	5.1	4.25	4	3.9
$q_e / \text{mg g}^{-1}$	34.45	63.66	75.39	80.46

154 *Morphological characterization of the ACs*

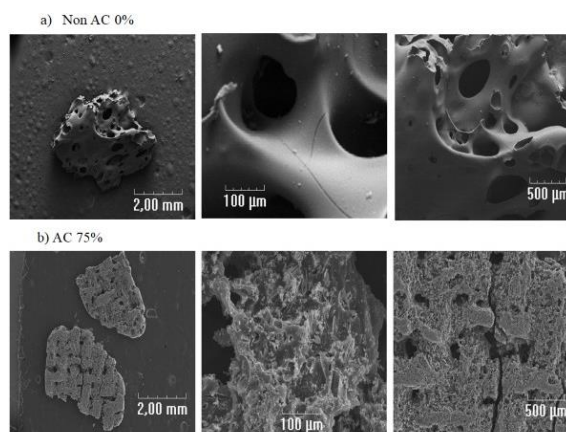
155 The scanning electron micrographs (SEM) of the non-activated carbon (non-
 156 -AC 0 %) and the AC 75 % are presented in Fig. 2a and b. The non-activated
 157 carbon (0 % H_3PO_4) and activated carbon (75 % H_3PO_4) samples derived from
 158 the polyester precursor show visible signs of fibers collapse and breakage, likely
 159 due to an intensified reaction with the polyester caused by the acid in the imp-
 160 -regnation stage and the pyrolysis temperature, with the woven form of the pre-
 161 -cursor is gone. Unlike carbon prepared from cotton, it has kept its woven and fib-
 162 -rous character,³ the polyester-derived carbon lost this structure.

163 It is also noticed that the porous structure (size of the pores) is well-developed,
 164 containing different sizes and shapes of pores which result from the activation
 165 process.

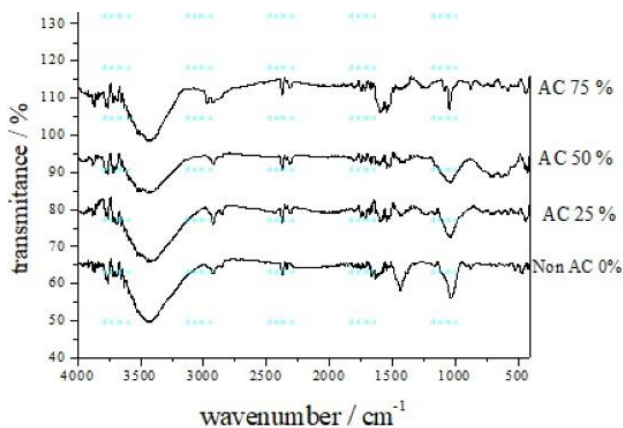
166 *FTIR analysis*

167 The FTIR spectra of the ACs prepared with different ratios (0, 25, 50 and 75
 168 %) are presented in Fig. 3. It is noted that the spectra corresponding to the different
 169 adsorbents are similar with respect to the type of functional groups. The difference

170 is only in the intensity of the peaks. The higher the activation rate, the more intense
 171 the peaks. Examination of all these spectra reveals the following absorption bands.



172
 173
 174 Fig. 2. SEM micrographs of: a) the non-activated carbon (0 % H₃PO₄) and
 b) the activated carbon (75 % H₃PO₄).



175
 176

Fig. 3. FTIR spectra of the carbon.

177 A broad absorption band observed between 3600–3300 cm⁻¹ with a maximum
 178 around 3400 cm⁻¹ is characteristic of the hydrogen elongation vibration of hydroxyl
 179 groups (of carboxyls, phenols or alcohols) and water adsorbed by the materials
 180 analyzed.¹⁶

181 The peaks at approximately 2300 and 2370 cm⁻¹ are characteristic of the C≡C
 182 stretching vibration of alkyne groups.¹⁷

183 The new band appearing in the AC 25 %, AC 50 % and AC 75 % around 1715
 184 and 1600 cm⁻¹ absent on the spectrum of non-AC 0 %, is most likely due to the

185 C=O indicating the formation of carbonyl-containing groups (ketones, aldehydes,
186 lactones, and carboxyl groups).¹⁸

187 The peak at 1556 cm^{-1} is characteristic of the C=O stretch of the carbonyl
188 group in a quinone and represents the γ -pyrone structure with strong vibrations
189 from a combination of C=O and C–C.¹⁹

190 The broad band at $1300\text{--}500\text{ cm}^{-1}$ was assigned to the C–O stretching and O–H
191 bending modes such as phenols, alcohols, esters and carboxylic acids.²⁰

192 The presence of hydroxyl groups of phenolic and carboxylic acids gives an
193 acidic character to the activated carbon surface whereas carbonyl and quinone
194 groups confer a basic character to the adsorbent surface.

195 The pH_{PZC} (Table I) shifted towards lower pH values when the impregnation
196 ratio increased due to the introduction of acidic groups.

197 *Effect of impregnation ratio on adsorption amount of clofibric acid*

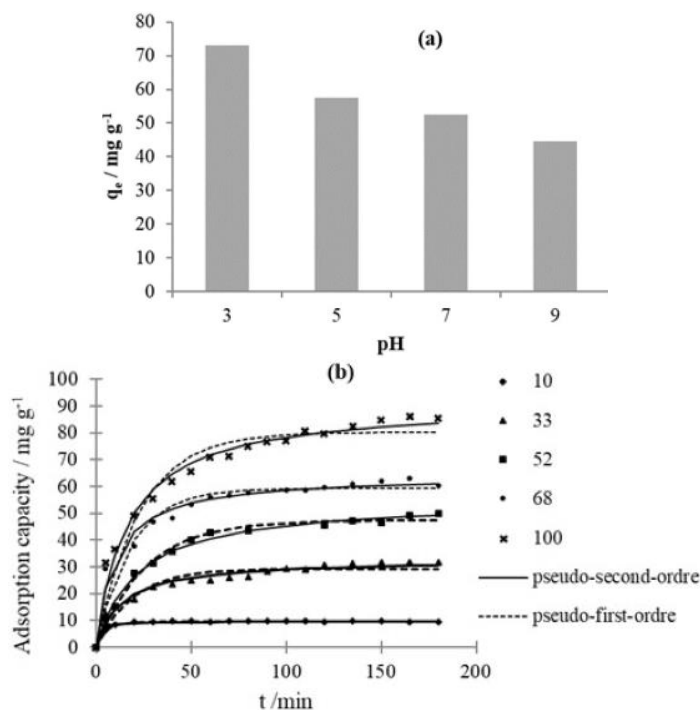
198 The impregnation ratio variation effect on the adsorption kinetics of the CA
199 onto activated carbon is presented in Table I. A higher elimination of CA is obs-
200 served when the impregnation ratio is increased from 0 to 75 % H_3PO_4 . The best
201 adsorption rate (% removal) of activated carbon obtained at 75 % phosphoric acid
202 was 80.46 mg g^{-1} . This may be attributed to the increase in adsorbent surface area,
203 microporosity development ($\approx 99\%$) and availability of more adsorption sites
204 resulting from the increase in impregnation ratio. Consequently, the activated car-
205 bon prepared with an activation ratio of 75 % H_3PO_4 was used in all subsequent
206 experiments.

207 *Effect of pH on the removal of clofibric acid*

208 pH is an important factor in any adsorption study. It can condition both the
209 surface charge of the adsorbent and the structure of the adsorbate. This quantity
210 characterizes the water, and its value will depend on the origin of the effluent. The
211 treatment technique to be adopted will strongly depend on the pH value. This is
212 the reason why, in any adsorption study, the influence of pH on the adsorption
213 capacity of a given solute on a specific adsorbent is essential.

214 The kinetic results of the adsorption of clofibric acid showed that the pH
215 studied in the range 3–9 is a critical factor. From Fig. 4a, it appears that CA
216 elimination is best at a very acidic pH (pH 3). The adsorption capacity gradually
217 decreases when the pH increases. It reaches its minimum at basic pH (pH 9). A
218 similar value was found in a previous study on the adsorption of clofibric acid by
219 an activated carbon prepared from cotton³.

220 The pH_{PZC} of AC 75 % is 3.9; thus, the surface carries a positive charge at
221 solution pH values less than 3.9, is neutral for $\text{pH} = \text{pH}_{\text{PZC}}$ and is negative for
222 solution pH values above 3.9.



223

224

225 Fig. 4. Adsorption of CA onto AC 75 % at different: a) initial pH; conditions: AC 75 %,
 226 agitation speed = 360 rpm and $T = 20^\circ\text{C}$ and b) contact time and initial CA concentration;
 227 conditions: AC 75 %, agitation speed = 360 rpm; $T = 20^\circ\text{C}$ and pH 3.

228 The increase of the CA adsorption capacity with increasing the acidic degree
 229 of the solution is attributed to the anionic and molecular forms of the CA and the
 230 positive surface charge of the activated carbon at lower pH. Therefore, the anionic
 231 form of CA is attracted by the positive charges of the activated carbon surface area.
 232 When the pH increases ($\text{pH} > \text{pH}_{\text{PZC}}$), the surface becomes more negatively
 233 charged and above the pK_a value clofibric acid is in the anionic form. This results
 234 in high electrostatic repulsions, leading to no significant adsorption.

235 *Effect of contact time and initial clofibric acid concentration*

236 One of the factors known to influence the amount of solute removed by
 237 adsorption is the adsorbent–adsorbate contact time. Therefore, we have monitored
 238 the CA adsorption capacity over a period of 3 h for different initial acid concentrations.

239 Fig. 4b indicates that equilibrium is almost reached after 60 min. It also shows
 240 that the adsorption takes place in two stages. At the start of the experiment, adsorption
 241 is rapid, which is due to the high availability of vacant active sites on the
 242 surface of the adsorbent. This step is followed by a second, slower step as there are
 243 fewer and fewer active sites to which clofibric acid can bind. The acid adsorption

244 capacity tends to stabilize, which is evidenced by the appearance of a plateau.
 245 Given these results, we set the duration of our experiences to 180 min to make sure
 246 there is no desorption of adsorbed molecules at contact times.

247 The influence of initial CA concentration on the adsorption capacity and
 248 kinetics is shown in Fig. 4b. The results show that the CA adsorption capacity
 249 increases with increasing initial solution concentration. This development can be
 250 explained by the existence of a strong gradient in the concentration of CA between
 251 the solution and the surface of the adsorbent when C_0 increases.

252 *Adsorption kinetics*

253 In order to examine the mechanism of the adsorption process, several models
 254 are given in the literature. We have tested three kinetic models in particular to
 255 analyze our experimental results: the pseudo-first-order model (Eq. (2)), the
 256 pseudo-second-order model (Eq. (3)) and the intra-particle diffusion model (Eq.
 257 (4)):³

$$258 \quad q_t = q_e(1 - e^{-k_1 t}) \quad (2)$$

$$259 \quad q_t = \frac{q_e^2 k_2 t}{1 + q_e k_2 t} \quad (3)$$

$$260 \quad q_t = x_i + k_d t^{0.5} \quad (4)$$

261 where q_e and q_t (mg g^{-1}) are the adsorption capacity at equilibrium and at time t ,
 262 respectively, k_1 (min^{-1}), k_2 ($\text{g mg}^{-1} \text{min}^{-1}$) and k_d ($\text{g mg}^{-1} \text{min}^{-1}$) are the rate
 263 constant of the pseudo-first-order, pseudo-second-order and intra-particle diffu-
 264 sion equations, respectively and x_i is the intercept of the straight line which is related
 265 to the boundary-layer thickness.

266 All the constants of the models tested (Table II) were determined by max-
 267 imizing the error function and using the solver add-in with Microsoft's spread-
 268 sheet, Microsoft Excel.²¹ The error function (coefficient of determination, R^2)
 269 employed was defined as follows:

$$270 \quad R^2 = \frac{\sum (q_{\text{cal}} - \bar{q}_t)^2}{\sum (q_{\text{cal}} - \bar{q}_t)^2 + \sum (q_{\text{cal}} - q_t)^2} \quad (5)$$

271 where q_{cal} and q_t both expressed in mg g^{-1} , represent the adsorption capacities of
 272 clofibric acid (CA) onto AC 75 % at time t . q_{cal} is obtained from the model, while
 273 q_t is determined experimentally. \bar{q}_t denotes the average of the experimental values
 274 (q_t).

275 According to Fig. 4b and the values of the parameters presented in Table II,
 276 based on the high R^2 and the difference between $q_{e(\text{cal})}$ and $q_{e(\text{exp})}$ values, the
 277 adsorption kinetics of CA onto AC 75 % is described by a pseudo-second-order

278 model. The matching adsorption process to the pseudo-second-order model indi-
 279 cates that various mechanisms such as chemisorption and diffusion into the pores
 280 contribute to the adsorption of CA onto active sites of the adsorbent.²²

281 TABLE II. Kinetic parameters for adsorption of CA onto AC 75 %; k_{d1} and k_{d2} in $\text{g mg}^{-1} \text{min}^{-1}$

Initial		Pseudo-first-order kinetics			Pseudo-second-order kinetics		
C_0 mg L^{-1}	$q_{e \text{ exp}}$ mg g^{-1}	$q_{e \text{ cal}}$ mg g^{-1}	k_1 L min^{-1}	R^2	$q_{e \text{ cal}}$ mg g^{-1}	k_2 $\text{g mg}^{-1} \text{min}^{-1}$	R^2
100	80.88	80.16	0.04	0.95	81	0.0007	0.98
68	59.37	59.21	0.056	0.94	58.85	0.0016	0.97
52	46.34	47.45	0.038	0.991	46.03	0.0008	0.994
33	30	29.33	0.05	0.93	30.04	0.002	0.97
10	9.6	9.56	0.21	0.996	9.62	0.07	0.999
Intra-particle diffusion							
$C_0 / \text{mg L}^{-1}$		k_{d1}	R^2	k_{d2}	R^2		
100		7.24	0.99	2.84	0.95		
70		4.95	0.98	1.06	0.80		
50		6.19	0.98	1.25	0.93		
30		2.36	0.99	1.28	0.96		
10		2.7	0.99	0.014	0.048		

282 Fig. S-1 of the Supplementary material to this paper shows two distinct linear
 283 segments, indicating a two-step adsorption process. The first linear portion
 284 corresponds to adsorption on the external surface (film diffusion), which is
 285 considered a fast step. The second portion is attributed to intra-particle diffusion,
 286 representing a slower phase of the adsorption process. The analysis of the intra-
 287 particle diffusion model (Table II) demonstrated that this diffusion is not the rate-
 288 limiting mechanism, and that diffusion through the boundary layer surrounding the
 289 adsorbent plays a non-negligible role.

290 *Adsorption isotherms*

291 Isotherms comprise an essential part of adsorption studies. From them, it is
 292 possible to evaluate the physical interactions between adsorbate and adsorbent.²³

293 In the present study, the Langmuir and Freundlich models (Table III) were
 294 tested by using the non-linear method to evaluate the adsorption capacity of our
 295 adsorbent and to determine the equilibrium isotherm. Fig. 5 shows the experi-
 296 mental data for the adsorption of CA on AC 75 % at different temperatures and the
 297 predicted equilibrium curves.

298 The adsorption isotherms obtained (Fig. 5) have a similar appearance and
 299 correspond to type L, according to the classification of Giles *et al.*²⁴ This type of
 300 isotherm suggests that the molecules adsorb flat on the surface of the adsorbent,
 301 and that there is no competition between clofibric acid and water molecules for the
 302 adsorption sites.

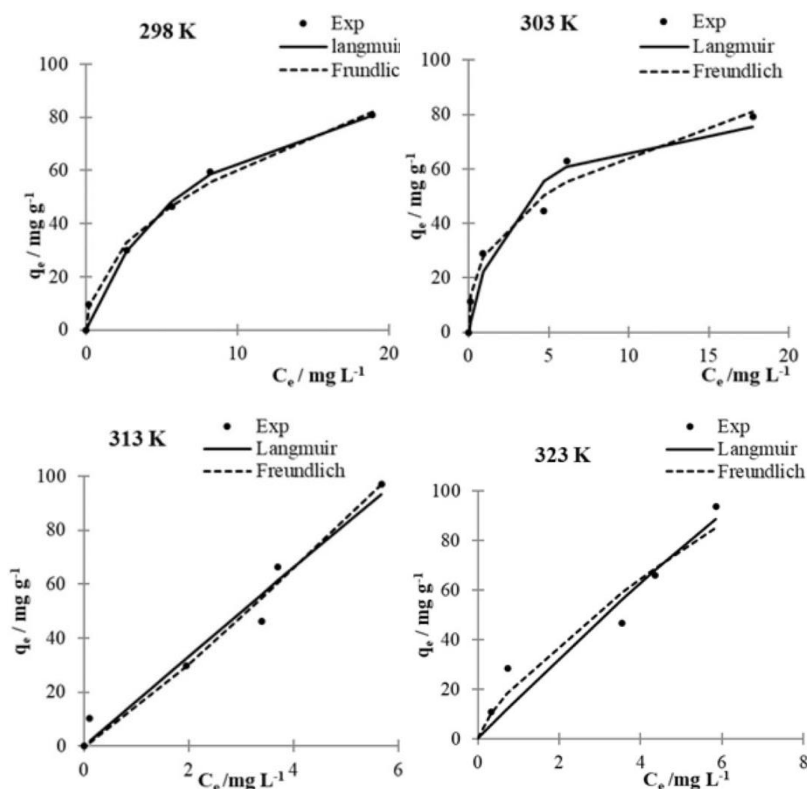


Fig. 5. Langmuir and Freundlich isotherms for the adsorption of CA onto AC75 % (conditions: 0.25 adsorbent, 250 mL of adsorbate solution, adsorption time 180 min, agitation speed 360 rpm, pH 3 and temperature 293–323 K).

It can be deduced (Fig. 5 and Table III) that the equilibrium data are well described by the Freundlich isotherm model.²⁵ The fitting results show that the value of n is superior to 2 at the temperatures of 293 and 303 K, indicating that the adsorption is good, while at 313 ($n = 0.9$) and 323 K ($n = 1.36$) adsorption is poor and moderately difficult, respectively.

A comparison is made between the adsorption capacity of AC 75 % for the removal of the pharmaceutical compound (CA) and other adsorbents reported in the literature. Mestre *et al.*²⁶ studied the adsorption of clofibric acid (pK_a 3.6) from aqueous solutions using two activated carbons derived from cork waste: CAC (chemically activated with K_2CO_3) and CPAC (physically activated from CAC *via* steam treatment). Textural analyses showed that CAC is predominantly microporous, with 68 % of its microporous volume consisting of narrow mesoporosity. CPAC had the highest specific surface area ($1060 \text{ m}^2 \text{ g}^{-1}$) and total porosity. Kinetic data were modeled using a pseudo-second-order kinetic model. The study demonstrated that pH significantly influenced clofibric acid adsorption, with peak

323 efficiency at pH 2, followed by progressive declines at pH 3.6 and 5. The sigmoidal
 324 adsorption isotherms were fitted with the Dubinin–Astakhov model, revealing a
 325 maximum adsorption capacity of 295 mg g⁻¹ for CPAC.

326 TABLE III. Parameters of the Langmuir and Freundlich models for the adsorption of CA onto
 327 ACC 75 %; q_m = maximum adsorption capacity; K_L = Langmuir constant; K_F and n =
 328 Freundlich constants

Model	Ref.	Parameter	293 K	303 K	313 K	323 K
Langmuir $q_t = \frac{q_m K_L C_e}{1 + K_L C_e}$	19	$q_m / \text{mg g}^{-1}$	112.71	86.94	3868	803.66
		$K_L / \text{L mg}^{-1}$	0.132	0.38	0.004	0.02
		R^2	0.98	0.95	0.96	0.94
Freundlich $q_e = K_L C_e^{1/n}$	19	$K_f / \text{mg}^{-1/n} \text{L}^{1/n}$	20.75	28.94	13.95	23.25
		$1/n$	0.47	0.36	1.11	0.73
		N	2.22	2.77	0.9	1.36
		R^2	0.99	0.97	0.97	0.95

329 Roza *et al.*²⁷ investigated the comparative adsorption behavior of ibuprofen
 330 (IBP) and clofibric acid (CA) onto activated carbon derived from bamboo waste,
 331 prepared by chemical activation with ZnCl₂ followed by microwave heating
 332 (ABW). Textural analyses revealed that ABW exhibits a porous structure combining
 333 micropores and mesopores (type II isotherm with a low-pressure hysteresis loop),
 334 and a specific surface area of 722.27 m² g⁻¹. The adsorption of both compounds
 335 was more effective under acidic conditions, particularly at pH values between 2
 336 and 5, due to favorable electrostatic interactions. The adsorption kinetics followed
 337 a pseudo-second-order model, suggesting that the process is governed by both
 338 chemical adsorption and intraparticle diffusion. The adsorption isotherms were
 339 best described by the Langmuir model, indicating monolayer adsorption, with
 340 maximum adsorption capacities of 278.55 mg g⁻¹ for IBP and 229.35 mg g⁻¹ for
 341 CA. The calculated Gibbs energy changes (-6.15 kJ mol⁻¹ for IBP and -5.56 kJ
 342 mol⁻¹ for CA) indicate that the adsorption processes are spontaneous and thermo-
 343 dynamically favorable.

344 Lu *et al.*²⁸ studied the adsorption and removal of clofibric acid (CA) and
 345 diclofenac (DCF) from water using a magnetic ion exchange (MIEX) resin. Ads-
 346 orption was found to be optimal within a pH range of 5 to 9, where both compounds
 347 predominantly exist in their anionic forms, thus favoring their exchange with the
 348 quaternary ammonium groups on the resin. The kinetic data primarily fit the
 349 pseudo-first-order model, and the study revealed that the process is jointly
 350 controlled by external mass transfer and surface diffusion. The maximum adsorp-
 351 tion capacities reported were 133.69 mg g⁻¹ for CA and 322.31 mg g⁻¹ for DCF.

352 Hasan *et al.*²⁹ investigated the removal of clofibric acid (CA) from water by
 353 adsorption using metal–organic frameworks (MOFs), particularly MIL-101, which
 354 they compared to activated carbon. MIL-101 exhibited a higher maximum adsorption

355 capacity (312 mg g^{-1} versus 244 mg g^{-1} for activated carbon), which was attri-
356 buted to its high specific surface area ($\sim 3100 \text{ m}^2 \text{ g}^{-1}$) and well-developed porosity.
357 The adsorption process followed a pseudo-second-order kinetic model, with equi-
358 librium reached more rapidly using MIL-101 than with the other adsorbents. Fur-
359 thermore, the adsorption was strongly pH-dependent: it was more effective under
360 acidic conditions, suggesting a favorable electrostatic interaction between the
361 anionic functional groups of CA and the cationic sites of the MOF.

362 A detailed comparison of all the discussed adsorbents is presented in Table S-I
363 of the Supplementary material.

364

CONCLUSION

365 This study demonstrated that polyester textile waste can be effectively val-
366 orized into high-performance adsorbent materials for the removal of the pharma-
367 ceutical pollutant, clofibric acid, present in wastewater. The adsorbent obtained
368 through chemical activation with phosphoric acid (H_3PO_4) followed by pyrolysis
369 at $600 \text{ }^\circ\text{C}$ resulted in a microporous activated carbon with a high specific surface
370 area (up to $826 \text{ m}^2 \text{ g}^{-1}$ for a 75 % impregnation ratio). Textural analyses (type I
371 isotherms) and morphological characterizations (SEM) confirmed the dominance
372 of microporosity, while FTIR spectroscopy revealed the presence of functional
373 groups (C=O, -OH) that enhance adsorption.

374 Adsorption tests showed:

- 375 – a removal efficiency greater than 95 % for low CA concentrations (10 mg
376 L^{-1}),
- 377 – adsorption kinetics described by the pseudo-second-order model, indi-
378 cating chemisorption-type interactions,
- 379 – optimal adsorption at pH 3, highlighting the importance of the carbon
380 surface charge and the ionic form of the pollutant,
- 381 – equilibrium data well-fitted by the Freundlich isotherm model, suggesting
382 heterogeneous adsorption on various types of sites and
- 383 – the most efficient sample corresponded to an impregnation ratio of 75 %
384 H_3PO_4 , for which the maximum measured adsorption capacity reached 80.46 mg
385 g^{-1} .

386 From an environmental perspective, this research offers an economical and
387 sustainable solution for managing textile waste and treating water contaminated
388 with pharmaceutical compounds. The produced ACs show promising potential for
389 large-scale applications, particularly in hospital or industrial wastewater treatment.

390

SUPPLEMENTARY MATERIAL

391 Additional data and information are available electronically at the pages of journal web-
392 site: <https://www.shd-pub.org.rs/index.php/JSCS/article/view/13381>, or from the correspond-
393 ing author on request.

394

ИЗВОД

395

АДСОРПЦИЈА КЛОФИБРИНСКЕ КИСЕЛИНЕ АКТИВНИМ УГЉЕМ ДОБИЈЕНИМ ОД
ОТПАДНЕ ПОЛИЕСТЕРСКЕ ТКАНИНЕ: ИСПИТИВАЊЕ ЕКСПЕРИМЕНТАЛНИХ
ПАРАМЕТАРА, КИНЕТИЧКЕ И АДСОРПЦИОНЕ РАВНОТЕЖЕ ПРИМЕНОМ
НЕЛИНЕАРНЕ МЕТОДЕ

396

397

398

399

NASSIMA BOUDRAHEM-BOUALIT^{1,2,3}, NABIL MAMERI³ и MOUNA CHALA¹

400

401

402

403

¹Laboratoire des Sciences et Techniques de l'Environnement, Ecole Nationale Polytechniques Alger, Avenue Pasteur El Harrach, 16110 Alger, Algeria, ²Faculté de Technologie, Université de Bejaia, Bejaia 06000, Algérie и ³Laboratoire de biotechnologie, Ecole Nationale Polytechniques Alger, Avenue Pasteur El Harrach, 16110 Alger, Algeria

404

405

406

407

408

409

410

411

412

413

414

Предмет овог истраживања је студија изводљивости припреме адсорбента од текстилног отпада (полиестера) за уклањање фармацеутских производа као што је клофибрина киселина (СА). Резултати су показали да су адсорбенти припремљени хемијском активацијом у присуству фосфорне киселине, а затим пиролизом на 600 °С, микропорозни материјали са великим специфичним површинама. Испитан је утицај времена контакта, почетне концентрације КА, рН раствора и температуре на адсорпцију. Процент уклањања КА из воденог раствора адсорпцијом већи од 95 % добијени су у случају разблажених раствора (10 mg L⁻¹) на собној температури и при рН 3. Кинетика адсорпције је успешно описана моделом псеудо-другог реда, а добијени изотерме су Фројндлиховог типа. Резултати указују да је овај процес спонтан, ефикасан и потенцијално применљив у уклањању СА из воде.

415

(Примљено 15. маја, ревидирано 25. јуна, прихваћено 6. августа 2025)

416

REFERENCES

417

418

419

420

421

422

423

424

425

426

427

428

429

430

431

432

433

434

435

436

437

438

439

1. A. V. Dordio, C. Duarte, M. Barreiros, A. J. P. Carvalho, A. P. Pinto, C. T. da Costa, *Bioresour. Technol.* **100** (2009) 1156 (<http://doi.org/10.1016/j.biortech.2008.08.034>)
2. V. Rakić, V. Rac, M. Krmar, O. Otman, A. Auroux, *J. Hazard. Mater.* **282** (2015) 141 (<http://doi.org/10.1016/j.jhazmat.2014.04.062>)
3. N. Boudrahem, F. Aissani-Benissad, F. Boudrahem, C. Vial, F. Audonnet, L. Favier, *Water Sci. Technol.* **82** (2020) 2513 (<http://doi.org/10.2166/wst.2020.524>)
4. M. E. Ramos, P. R. Bonelli, S. Blacher, M. M. L. Ribeiro Carrott, P. J. M. Carrott, A. L. Cukierman, *Colloids Surfaces, A* **378** (2011) 87 (<http://doi.org/10.1016/j.colsurfa.2011.02.005>)
5. Y. Sun, Q. Yue, B. Gao, Q. Li, L. Huang, F. Yao, X. Xu, *J. Colloid Interface Sci.* **368** (2012) 521 (<http://doi.org/10.1016/j.jcis.2011.10.067>)
6. A. C. Pastor, F. Rodríguez-Reinoso, H. Marsh, M. A. Martínez, *Carbon* **37** (1999) 1275 ([http://doi.org/10.1016/S0008-6223\(98\)00324-8](http://doi.org/10.1016/S0008-6223(98)00324-8))
7. C. F. Brasquet, B. Bourges, P. L. Cloirec, *Environ. Sci. Technol.* **33** (1999) 4226 (<https://doi.org/10.1021/es981358m>)
8. C. F. Brasquet, P. L. Cloirec, *Langmuir* **15** (1999) 5906 (<https://doi.org/10.1021/la9811160>)
9. E. Ayranci, O. Duman, *J. Hazard. Mater.* **124** (2005) 125 (<https://doi.org/10.1016/j.jhazmat.2005.04.020>)
10. J. R. Rangel-Mendez, M. Streat, *Water Res.* **36** (2002) 1244 ([https://doi.org/10.1016/S0043-1354\(01\)00343-8](https://doi.org/10.1016/S0043-1354(01)00343-8))
11. M. A. Álvarez-Merino, V. López-Ramón, *J. Colloid Interface Sci.* **288** (2005) 335 (<https://doi.org/10.1016/j.jcis.2005.03.025>)

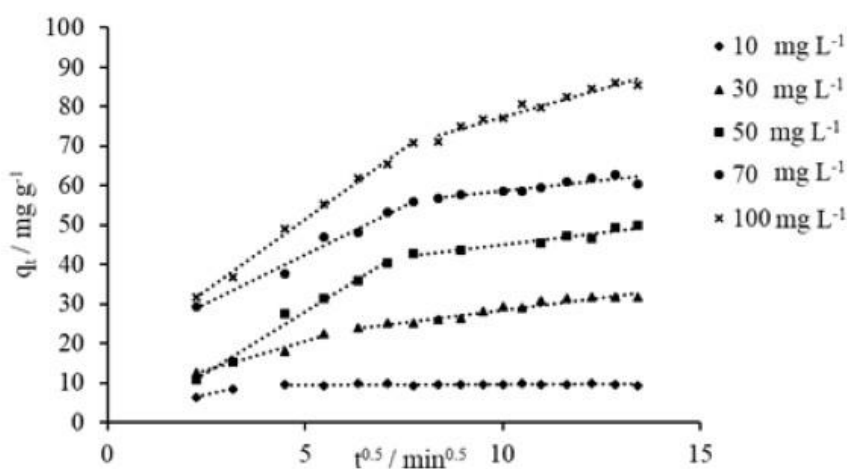
- 440 12. F. Akkouche, F. Boudrahem, I. Yahiaoui, C. Vial, F. Audonnet, F. Aissani-Benissad,
441 *Water Environ. Res.* **39** (2021) 464 (<https://doi.org/10.1002/wer.1449>)
- 442 13. L. Khenniche, F. Aissani, *J. Chem. Eng. Data* **55** (2010) 728
443 (<http://doi.org/10.1021/je900426a>)
- 444 14. Y. Guo, D. A. Rockstraw, *Carbon* **44** (2006) 1464
445 (<http://doi.org/10.1016/j.carbon.2005.12.002>)
- 446 15. M. E. Ramos, P. R. Bonelli, A. L. Cukierman, *Colloids Surfaces A* **324** (2008) 86
447 (<https://doi.org/10.1016/j.colsurfa.2008.03.034>)
- 448 16. Y. Chen, S. R. Zhai, N. Liu, Y. Song, Q. Da An, X. W. Song, *Bioresour. Technol.* **144**
449 (2013) 401 (<http://doi.org/10.1016/j.biortech.2013.07.002>)
- 450 17. I. I. Gurten, M. Ozmak, E. Yagmur, Z. Aktas, *Biomass Bioenergy* **37** (2012) 73
451 (<https://doi.org/10.1016/j.biombioe.2011.12.030>)
- 452 18. K. Y. Foo, B. H. Hameed, *Chem. Eng. J.* **180** (2012) 66
453 (<http://doi.org/10.1016/j.cej.2011.11.002>)
- 454 19. J. Zheng, Q. Zhao, Z. Ye, *Appl. Surf. Sci.* **299** (2014) 86
455 (<http://doi.org/10.1016/j.apsusc.2014.01.190>)
- 456 20. S. M. Yakout, G. Sharaf El-Deen, *Arab. J. Chem.* **9** (2016) S1155
457 (<http://doi.org/10.1016/j.arabjc.2011.12.002>)
- 458 21. N. Boudrahem, S. Delpoux-Ouldriane, L. Khenniche, F. Boudrahem, F. Aissani-Benissad,
459 M. Gineys, *Process Saf. Environ. Prot.* **111** (2017) 544
460 (<http://doi.org/10.1016/j.psep.2017.08.025>)
- 461 22. K. Yahiaoui, F. Boudrahem, S. Ziani, I. Yahiaoui, F. Aissani-Benissad, *Int. J. Environ.*
462 *Anal. Chem.* **102** (2022) 6670 (<http://doi.org/10.1080/03067319.2020.1814272>)
- 463 23. P. Del Vecchio, N. K. Haro, F. S. Souza, N. R. Marcílio, L. A. Féris, *Water Sci. Technol.*
464 **79** (2019) 2013 (<http://doi.org/10.2166/wst.2019.205>)
- 465 24. C. H. Giles, T. H. MacEwan, S. N. Nakhwa, D. Smith, *J. Chem. Soc.* **846** (1960) 3973
466 (<http://doi.org/10.1039/JR9600003973>)
- 467 25. F. Boudrahem, F. Aissani-Benissad, A. Soualah, *Desalin. Water Treat.* **54** (2015) 1727
468 (<http://doi.org/10.1080/19443994.2014.888686>)
- 469 26. A. S. Mestre, M. L. Pinto, J. Pires, J. M. F. Nogueira, A. P. Carvalho, *Carbon* **48** (2010)
470 972 (<http://doi.org/10.1016/j.carbon.2009.11.013>)
- 471 27. R. A. Reza, M. Ahmaruzzaman, A. K. Sil, V. K. Gupta, *Ind. Eng. Chem. Res.* **53** (2014)
472 9331 (<http://doi.org/10.1021/ie404162p>)
- 473 28. X. Lu, Y. Shao, N. Gao, J. Chen, Y. Zhang, Q. Wang, Y. Lu, *Chemosphere* **161** (2016)
474 400 (<http://doi.org/10.1016/j.chemosphere.2016.07.025>)
- 475 29. Z. Hasan, J. Jeon, S. H. Jhung, *J. Hazard. Mater.* **209–210** (2012) 151
476 (<http://doi.org/10.1016/j.jhazmat.2012.01.005>).

477 SUPPLEMENTARY MATERIAL TO
 478 **Adsorption of clofibric acid on the activated carbon prepared**
 479 **from polyester cloth waste: Study of the operational parameters,**
 480 **kinetics and adsorptive equilibrium using the non-linear method**

481 NASSIMA BOUDRAHEM-BOUALIT^{1-3*}, NABIL MAMERI³ and MOUNA CHALA¹

482 ¹Laboratoire des Sciences et Techniques de l'Environnement, Ecole Nationale Polytechniques
 483 Alger, Avenue Pasteur El Harrach, 16110 Alger, Algeria, ²Faculté de Technologie, Université
 484 de Bejaia, Bejaia 06000, Algeria and ³Laboratoire de biotechnologie, Ecole Nationale
 485 Polytechniques Alger, Avenue Pasteur El Harrach, 16110 Alger, Algeria

486 J. Serb. Chem. Soc. 91 (0) (2026) 000–000



487
 488 Fig. S-1. Kinetics intra-particle diffusion of CA adsorption on AC 75% with different initial
 489 concentrations. Conditions: AC 75%, pH = 3, agitation speed = 360 rpm and T = 20 °C.

490

* Corresponding author. E-mail: nassima.boudrahem@g.enp.edu.dz

491 TABLE S-I. Comparison of adsorption capacities for the removal of CA from aqueous solutions
 492 using other adsorbents.

Study	Adsorbent used	Preparation / activation	S_{BET} (m^2g^{-1})	Optimal pH	Kinetic model	Isotherm model	q_{max} (mg g^{-1})	Remarks
Present study	Activated carbon from polyester textile waste	H_3PO_4 activation + pyrolysis at 600°C	826	3	Pseudo-second order	Freundlich	80.46	Low-cost, sustainable solution, high efficiency at low conc.
Mester et al. ²⁶	CAC, CPAC	Cork waste + K_2CO_3 (chemical) / steam (physical)	1060 (CPAC)	2	Pseudo-second order	Dubinin–Astakhov	295	High-performance materials, large adsorption capacity
Roza et al. ²⁷	Bamboo-based activated carbon (ABW)	ZnCl_2 activation + microwave heating	722.27	2-5	Pseudo-second order	Langmuir	229.35	Micro-/mesoporous structure, monolayer adsorption, high capacity
Lu et al. ²⁸	MIEX resin (ion exchange)	Synthesized magnetic resin	Not specified	5-9	Pseudo-first order	Langmuir	133.69	Ion exchange mechanism, good performance at neutral/basic pH
Hasan et al. ²⁹	Metal-Organic Framework (MIL-101)	MOF synthesis	3100	< 5	Pseudo-second order	Langmuir	312	Highly efficient material, but costly and complex to produce